

# dc superconducting quantum interference device based neodymium magnet displacement sensor for superfluid experiments

Yuki Sato and Richard Packard

Department of Physics, University of California at Berkeley, Berkeley, California 94720, USA

(Received 24 March 2009; accepted 15 April 2009; published online 5 May 2009)

A new displacement sensor that uses a rare-earth magnet attached to a flexible diaphragm is demonstrated for superfluid experiments. Its construction, calibration, and performance are described. © 2009 American Institute of Physics. [DOI: 10.1063/1.3129942]

## I. INTRODUCTION

Diaphragm displacement sensors are often used in low temperature environments. The most sensitive such sensors employ superconducting quantum interference device (SQUID) technology. For example, to monitor superfluid motion in weak link experiments, we and others have employed circuits similar to that invented by Paik.<sup>1</sup> This Paik system uses a persistent current trapped in a SQUID circuit, and the motion of a superconducting metal-coated diaphragm changes the inductance of the circuit and registers a signal in a SQUID. We describe here the performance of a much simplified sensor that eliminates the persistent current and its associated persistent current switches.

The Paik-type transducer circuit used in our previous experiments is shown in Fig. 1(a) and described in detail in Ref. 2. A persistent current of the order of  $\sim 1$  A is trapped in the lower part of the circuit using a pair of persistent current switches. There are six superconducting joints required to build the circuit. The failure of any one joint renders the device inoperative. Setting the persistent current employs three power supplies: two for the heaters and one to initiate the persistent current. As many as six low temperature leads are required to carry the associated currents. These leads require careful heat sinking to avoid heat leaks, especially if the circuit is used at millikelvin temperatures. Mechanical switches are often used in the cryogenic environment in the current injection line (that extends to the top of the cryostat) to eliminate as much electrical noise pickup as possible. The diaphragm is coated with a superconducting film, and its motion (due to superfluid flow coupled to the diaphragm) changes the inductance of the nearby pancake-shaped pickup coil. Flux conservation induces finite current in the top half of the circuit, which is then detected and converted to voltage by a dc SQUID. Typical displacement resolution for this type of sensor has been  $\sim 3 \times 10^{-15}$  m/ $\sqrt{\text{Hz}}$ .

The new displacement sensor described here uses a small rare-earth magnet attached to a diaphragm. The magnet's field creates a flux in the input coil of a dc SQUID. The circuit is shown in Fig. 1(b), and the experimental cell is depicted schematically in Fig. 2. When the diaphragm changes position, the field from the magnet changes the flux in the pickup coil. The SQUID electronics outputs a voltage

linear in the displacement of the diaphragm. A similar displacement sensor has been employed in Mossbauer redshift experiment<sup>3</sup> and torsional oscillator experiment,<sup>4</sup> and we have applied the same principle for the use with superfluid experiments. The simple circuit, which involves only the SQUID input leads, uses no persistent current joints and no external power supplies. The entire system sits in a cryogenic environment, which eliminates electric and acoustic noise injected from the outside. We describe the construction, calibration, and performance of the device. We show that it can be used successfully in superfluid experiments by detecting the characteristic dynamic behaviors of superfluid <sup>4</sup>He such as the so-called Helmholtz mode<sup>5</sup> and Josephson oscillations.<sup>5-7</sup>

## II. EXPERIMENTAL CELL CONSTRUCTION

### A. Pickup coil

Our pickup coil is made of five turns (single layer) of 0.1 mm OD NbTi wire wound flat around a 0.5 mm OD post. The outer diameter of this “pancake” coil is  $\sim 1.6$  mm. The wire is wound on a former made of 1266 Stycast,<sup>8</sup> and the former (with the coil glued onto it with the same Stycast) is held in a sleeve (made of 2850FT Stycast<sup>8</sup>) so that the surface of the coil is flush with that of the sleeve. The sleeve is inserted in a brass holder and glued with 2850FT Stycast [see Fig. 3(a)]. The leads from the pickup coil are twisted and inserted in a Pb tube to exclude changing magnetic flux.

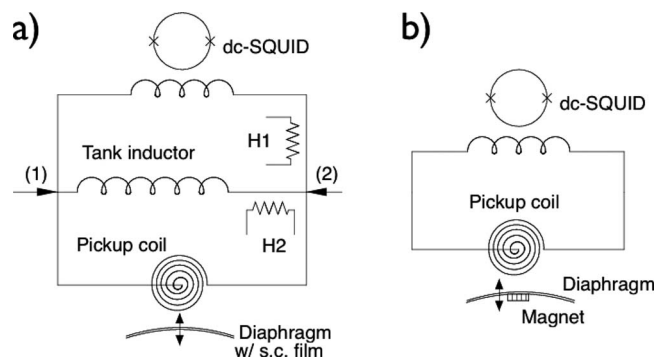


FIG. 1. (a) Conventional displacement sensor circuit. H1 and H2 are persistent current switches, and leads (1) and (2) are used for current injection. (b) Magnet displacement sensor circuit.

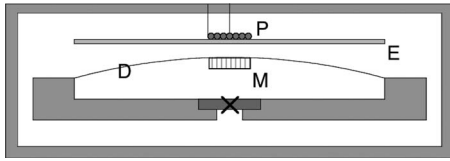


FIG. 2. Cell schematic. D: diaphragm (metallized), E: electrode, P: pickup coil (connected to a commercial dc SQUID outside of experimental cell), M: magnet. X indicates a superfluid Josephson junction.

## B. Magnet

The magnet used is a N50 grade neodymium (NdFeB) magnet<sup>9</sup> ( $\sim 1.6$  mm OD and  $\sim 0.8$  mm thick, magnetized in axial direction). Its nominal weight is 0.0118 g, and the surface field strength is specified as 0.18 T.

## C. Diaphragm and electrode

The magnet is glued onto the back of a  $\sim 7.6$   $\mu\text{m}$  thick Kapton diaphragm<sup>10</sup> with a thin layer of 1266 Stycast [see Fig. 4(a)]. The other side of the diaphragm is coated with a layer ( $\sim 140$  nm in thickness) of aluminum. The evaporated metal should be normal (rather than superconducting) for the sensor to work. Since our present experiments are done above 2 K, the evaporated film remains normal. A thin aluminum film has a rather broad superconducting transition temperature around 1.5 K depending on exact evaporation methods used,<sup>11</sup> and one should be careful if aluminum is used near this temperature range. The diaphragm is glued at the edges onto the main cell with 1266 Stycast in such a way that the center region remains flexible (see Fig. 2).

The electrode is constructed similarly by evaporating aluminum ( $\sim 140$  nm in thickness) on a  $\sim 7.6$   $\mu\text{m}$  thick Kapton sheet. The Kapton sheet is then glued onto the pickup coil described above with a thin layer of 1266 Stycast (see Fig. 3(b)). Electrical connections to the diaphragm and the electrode are made with evaporated tabs to which wires are connected with screw press joints.

The electrode and the diaphragm are placed together with  $\sim 76$   $\mu\text{m}$  Kapton spacers. Once the experimental cell is filled with superfluid  $^4\text{He}$ , we apply a voltage between the diaphragm and the electrode to pull up on the diaphragm, driving superfluid flow through a nanoscale aperture array (shown as X in Fig. 2). An array of nanoscale apertures exhibits<sup>6,7</sup> Josephson phenomena near the transition temperature in superfluid  $^4\text{He}$ . A  $150 \times 150$  array of nominally 70 nm holes spaced 1  $\mu\text{m}$  apart from each other (made in a

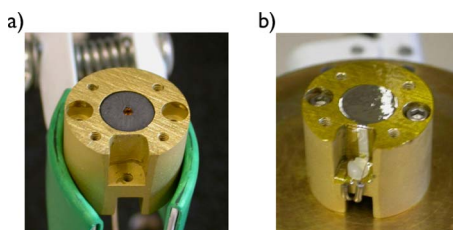


FIG. 3. (Color online) (a) Pickup coil can be seen at the center of black Stycast. (b) Electrode is glued onto the pickup coil.

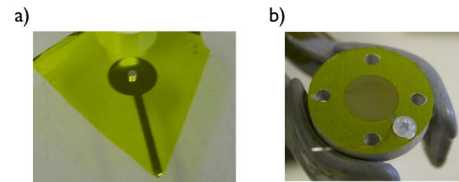


FIG. 4. (Color online) (a) Magnet is glued to the back of a diaphragm. (b) Diaphragm is glued to the main cell piece, which houses the superfluid Josephson junction.

$\sim 60$  nm thick SiN membrane) is installed in this experimental cell. The electrode and the diaphragm are also used to do capacitive measurements.

## III. CALIBRATION

### A. Displacement sensor output vs bias voltage

The force on the diaphragm (of area  $A$ ) due to a bias voltage  $V_b$  applied between it and the electrode is

$$F = \frac{d}{dx} \left( \frac{1}{2} C_m V_b^2 \right) = - \frac{1}{2d} C_m V_b^2, \quad (1)$$

where  $C_m = \epsilon A / d$  is the capacitance between the diaphragm and the electrode, and  $d$  is the distance between them. This allows us to write

$$k(\Delta x + x_0) = - \frac{\epsilon A}{2d^2} (V_b - V_0)^2, \quad (2)$$

where  $k$  is the spring constant of the diaphragm and  $\Delta x$  is the displacement of the diaphragm from its equilibrium position. Then

$$\Delta x = - \frac{\epsilon A}{2kd^2} (V_b - V_0)^2 - x_0. \quad (3)$$

We define the sensitivity  $s$  of the displacement sensor as

$$\Delta V_{\text{SQ}} = s \Delta x, \quad (4)$$

where  $\Delta V_{\text{SQ}}$  is the SQUID output voltage in a circuit shown in Fig. 1(b). Using this,

$$\Delta V_{\text{SQ}} = - \beta_1 V_b^2 + 2\beta_1 V_b V_0 - \beta_1 V_0^2 - s x_0, \quad (5)$$

where  $\beta_1 \equiv \epsilon s A / 2kd^2$ . This  $\beta_1$  can be determined by applying bias voltages to the diaphragm and fitting the SQUID output to the parabolic form above. A typical measurement (done at  $T \sim 2.06$  K with experimental cell full of superfluid  $^4\text{He}$ ) is shown in Fig. 5. This yields  $\beta_1 \approx 4.67 \times 10^{-2} [1/\text{V}]$ .

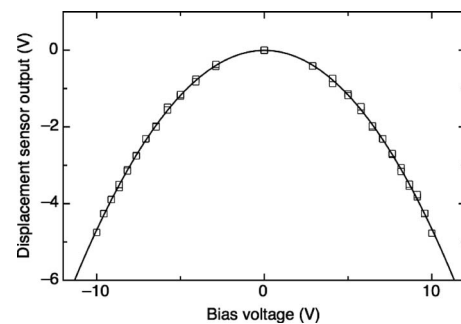


FIG. 5. Displacement sensor output vs bias voltage. Solid line is a fit.

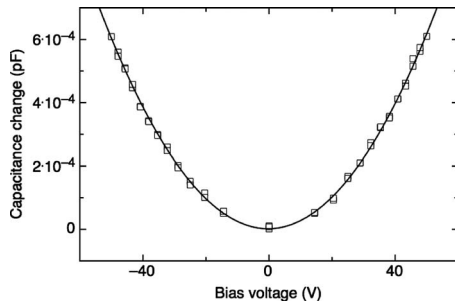


FIG. 6. Capacitance change vs bias voltage. Solid line is a fit.

## B. Capacitance change vs bias voltage

Here we assume that the change in diaphragm position is related to the change in capacitance (between the diaphragm and the electrode) by

$$\frac{\Delta x}{d} \approx \frac{\Delta C_m}{C_m}. \quad (6)$$

Applying this to Eq. (2) gives

$$\Delta C_m = \beta_2 V_b^2 - 2\beta_2 V_b V_0 + (2k\beta_2)^{1/2} x_0 + \beta_2 V_0^2, \quad (7)$$

where  $\beta_2 = \varepsilon^2 A^2 / 2kd^4$ . This  $\beta_2$  can be determined by applying bias voltages to the diaphragm and fitting the change in capacitance (measured with a capacitance bridge) to the form above. A measurement (done at  $T \sim 2.06$  K with experimental cell full) is shown in Fig. 6. This yields  $\beta_2 \approx 2.44 \times 10^{-7}$  [pF/V<sup>2</sup>].

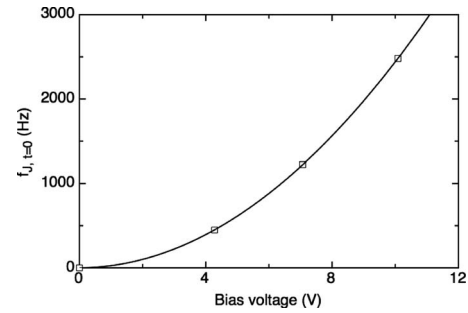
## C. Josephson frequency relation

When a constant chemical potential difference  $\Delta\mu$  is applied across the weak links near  $T_\lambda$ , a mass current through the aperture array oscillates<sup>5-7</sup> at the Josephson frequency  $f_J = \Delta\mu/h$ . For superfluid <sup>4</sup>He,  $\Delta\mu = m_4(\Delta P/\rho - s\Delta T)$ , where  $\Delta P$  and  $\Delta T$  are pressure and temperature differentials,  $\rho$  is the mass density,  $s$  is the specific entropy, and  $m_4$  is the <sup>4</sup>He atomic mass. We use this relation to obtain the distance between the electrode and the diaphragm rather than using the nominal design value of  $d \approx 76$   $\mu\text{m}$  for further calibration.

When we apply a step voltage  $V_b$  between the diaphragm and the electrode, a step pressure  $\Delta P = \varepsilon V_b^2 / 2d^2$  is created across the aperture array. The temperatures on either side of the junction are equal ( $\Delta T = 0$ ) at this initial instant of time, and the entire chemical potential difference is determined by the initial pressure step. Therefore, at temperatures sufficiently close enough to  $T_\lambda$  ( $T_\lambda - T \leq 3$  mK in this experiment), we can drive the Josephson mass current oscillation, and it starts at frequency  $f_{J,t=0} = m_4 \Delta P / \rho h$ . This gives

$$\frac{\varepsilon}{2d^2} (V_b - V_0)^2 = \frac{f_{J,t=0} \rho h}{m_4}. \quad (8)$$

Then measuring  $f_{J,t=0}$  for various bias voltages and fitting to the form above gives a measurement of  $d$ . Such measurement (shown in Fig. 7) gives  $d \approx 114$   $\mu\text{m}$ .

FIG. 7. Josephson oscillation frequency at  $t=0$  vs bias voltage applied to drive the oscillation.

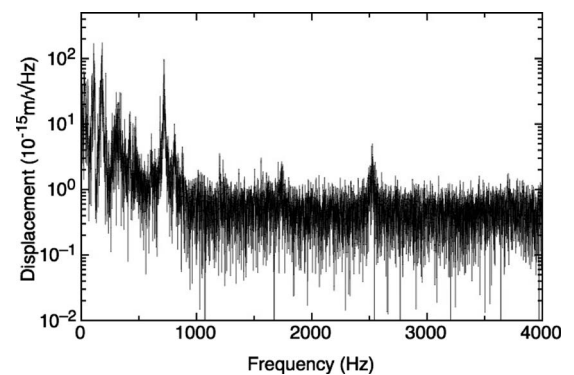
## IV. PERFORMANCE

### A. Sensitivity

The measured values for  $\beta_1$ ,  $\beta_2$ , and  $d$  give the displacement sensor sensitivity  $\varsigma \sim 7 \times 10^9$  [V/m] and spring constant  $k \sim 2.6 \times 10^3$  [N/m]. A typical noise spectrum with the experimental cell full of superfluid <sup>4</sup>He is shown in Fig. 8. Peaks are acoustic resonances associated with the experimental cell. Away from a background peak the displacement resolution above  $f \sim 1$  kHz is  $\sim 1 \times 10^{-15}$  m/ $\sqrt{\text{Hz}}$ , which is several times better than what we typically observe with the previous (and more complex) technique. The device sensitivity and the displacement resolution can be easily improved even further with more turns in the pickup coil and by using a stronger magnet. However the vibration isolation must also be improved to make such a sensitive sensor useful in experiments. The transducer sensitivity of  $\varsigma \sim 7 \times 10^9$  [V/m] is ideal for maximizing the signal and yet keeping it in the SQUID dynamic range for our current experiments. The advantage of this particular displacement sensor is the sensitivity and the simplicity of the design that makes the construction quite straightforward.

### B. Detecting the dynamic behaviors of superfluid <sup>4</sup>He

For many experiments the sensor and the technique described here may be used simply to measure a direct displacement. However in our particular application, we need to use the diaphragm motion to track the movement of superfluid helium in an aperture array, which is hydraulically

FIG. 8. Spectrum taken at  $T \sim 2.06$  K with experimental cell full.

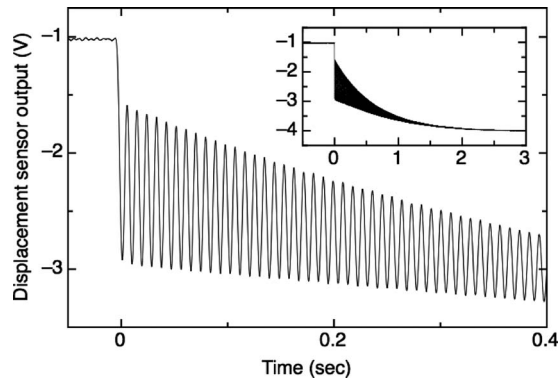


FIG. 9. Helmholtz mode. Bias voltage is applied at time=0. The inset shows the overall transient behavior. Data taken at  $T \sim 2.06$  K. Frequency is  $\sim 108$  Hz.

coupled to the diaphragm. To confirm that the new displacement sensor can be used effectively in superfluid experiments, one needs to see if it can detect the characteristic behaviors that have been detected and studied in the past. When an experimental cell, such as the one depicted in Fig. 2, is filled with superfluid  $^4\text{He}$ , there is a resonant mode (often called the Helmholtz mode) associated with it. The restoring force of the diaphragm, the inertia of the fluid moving in the apertures, and the heat capacity of the fluid in the inner cell volume determine the resonant frequency.<sup>12</sup> Figure 9 is an example of a time trace of the displacement sensor output where we apply a step voltage between the diaphragm and the electrode at  $t=0$ . The resonant mode is apparent in the figure. We have compared the shape of the oscillation in time as well as frequency and quality factor of the mode as functions of temperature with those obtained in previous experimental runs,<sup>5-7</sup> and have not found any noticeable effects from having a mass (magnet) attached to the diaphragm.

One may compare the kinetic energy of the fluid within the apertures and that of a moving diaphragm with a magnet attached to it. For the fluid flowing in the aperture array, we can approximate the typical kinetic energy to be

$$\text{KE}_f \sim \frac{1}{2} m v_f^2 \sim \frac{1}{2} (\rho_s N a l) v_f^2,$$

where  $\rho_s$  is the superfluid density,  $N$  is the number of apertures,  $a$  is the aperture area,  $l$  is the aperture length, and  $v_f$  is the fluid velocity. To conserve mass,  $\rho A v_d \sim \rho_s v_f N a$ , where  $v_d$  is the diaphragm velocity.

The kinetic energy of the diaphragm is

$$\text{KE}_d \sim \frac{1}{2} (m_d + m_M) v_d^2 \sim \frac{1}{2} (m_d + m_M) (\rho_s v_f N a / \rho A)^2,$$

where  $m_d$  is the diaphragm mass and  $m_M$  is the magnet mass. Using this, the ratio of energies is

$$\text{KE}_d / \text{KE}_f \sim (m_d + m_M) N a \rho_s / \rho^2 A^2 l.$$

Since the mass of the magnet  $m_M (\sim 12 \times 10^{-3}$  g) is much bigger than that of the diaphragm  $m_d (\sim 0.6 \times 10^{-3}$  g), we can replace  $m_d + m_M$  with just  $m_M$  in the equation above. Using the numbers,  $N = 150 \times 150$ ,  $a \sim (70 \text{ nm})^2$ ,  $\rho \sim 146 \text{ kg/m}^3$ ,  $A \sim 0.5 \text{ cm}^2$ ,  $l \sim 60 \text{ nm}$ ,  $m_M \sim 12 \times 10^{-3}$  g, and  $\rho_s \sim 146 \text{ kg/m}^3$  (at  $T \sim 1.5$  K), we obtain  $\text{KE}_d / \text{KE}_f \sim 0.06$ . [This ratio even decreases to  $\sim 0.004$  at  $T_\lambda - T \sim 10$  mK (with  $\rho_s \sim 10 \text{ kg/m}^3$ ) approximately where we

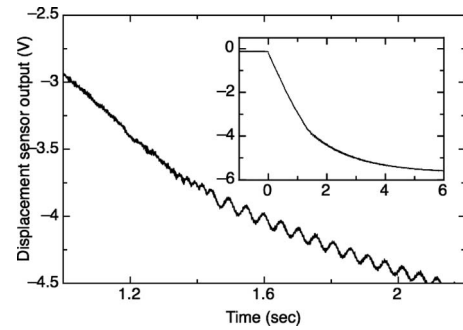


FIG. 10. Individual phase slips have been detected with the new sensor. Phase slip oscillation ends and the Helmholtz mode begins at time  $\sim 1.42$  sec. Data taken at  $T_\lambda - T \sim 1$  mK.

usually do our Josephson experiments.] Therefore the kinetic energy associated with the fluid flow in the aperture array dominates over that of the moving diaphragm even with the magnet attached to it. Then the notion that the diaphragm can be approximated as an energy-storing device in the hydrodynamic picture<sup>13</sup> of the cell is still valid, and this is why the sensor signal does not show any noticeable effects from having a magnet attached to the diaphragm.

We have also used the new sensor to detect Josephson oscillations near the superfluid transition temperature. Individual phase slip events can be seen in Fig. 10. (Details on phase slip oscillation are discussed in Refs. 5 and 7.)

## V. CONCLUSION

We have described the design, construction, and calibration of a SQUID-based neodymium magnet displacement sensor and demonstrated its performance in superfluid Josephson weak link experiments. The displacement resolution is  $\sim 1 \times 10^{-15}$  m/ $\sqrt{\text{Hz}}$  for frequencies 1 kHz and above. This resolution is about three times better than what we typically obtain with the previous technique, and the experimental signal is kept well within the SQUID dynamic range. Construction is much simpler with the new device. Mass loading the diaphragm with a magnet does not seem to affect the sensing capability, and the superfluid dynamics seems unaltered by it. The sensitivity can easily be improved further for experiments that require it as long as the system is well isolated from external vibration.

## ACKNOWLEDGMENTS

We thank Erkki Ikonen and John Clarke for helpful discussions. Aperture arrays were fabricated by Aditya Joshi at Cornell Nanoscale Facility, a member of the NSF National Nanotechnology Infrastructure Network. This work was supported by the ONR (Grant No. N00014-06-1-1183) and by the NSF (Grant No. DMR 0244882).

<sup>1</sup>H. J. Paik, *J. Appl. Phys.* **47**, 1168 (1976).

<sup>2</sup>O. Avenel and E. Varoquaux, *Proceedings of the 11th International Cryogenic Engineering Conference*, Berlin, edited by G. Klipping and I. Klipping (Butterworths, Guildford, 1986), p. 587.

<sup>3</sup>E. Ikonen, H. Seppa, W. Potzel, and C. Schafer, *IEEE Trans. Instrum. Meas.* **40**, 196 (1991).

<sup>4</sup>S. Davis, private communication.

<sup>5</sup>Y. Sato, E. Hoskinson, and R. E. Packard, *Phys. Rev. B* **74**, 144502 (2006).

<sup>6</sup>E. Hoskinson, R. E. Packard, and T. Haard, *Nature (London)* **433**, 376 (2005).

<sup>7</sup>E. Hoskinson, Y. Sato, I. Hahn, and R. E. Packard, *Nat. Phys.* **2**, 23 (2006).

<sup>8</sup>Ellsworth Adhesives, W129N10825 Washington Dr. Germantown, WI 53022 USA.

<sup>9</sup>K&J Magnetics, Inc, 2110 Ashton Dr. Jamison, PA 18929 USA.

<sup>10</sup>Dupont, <http://www.dupont.com/kapton/>.

<sup>11</sup>T. A. Moreau and R. B. Hallock, *J. Low Temp. Phys.* **127**, 189 (2002).

<sup>12</sup>E. Hoskinson, Ph.D. thesis, University of California at Berkeley, 2005.

<sup>13</sup>S. Backhaus, Ph.D. thesis, University of California at Berkeley, 1997.